Journal of Electroceramics, 8, 57–64, 2002

Electrochemical Gas Sensor Materials Studied by Impedance Spectroscopy Part II: Reference Electrode and Solid Electrolyte/Electrode System

P. PASIERB,* S. KOMORNICKI, R. GAJERSKI & S. KOZIŃSKI
Faculty of Materials Science and Ceramics, University of Mining and Metallurgy, 30-059 Cracow, Poland

P. TOMCZYK
Faculty of Fuels and Energy, University of Mining and Metallurgy, 30-059 Cracow, Poland

M. RĘKAS
School of Materials Science and Engineering, The University of New South Wales, UNSW Sydney, NSW 2052, Australia

Submitted August 6, 2001; Revised February 6, 2002; Accepted February 12, 2002

Abstract. The behavior of the reference electrode ($Na_2Ti_6O_{13}$—TiO_2) and the electrode/solid electrolyte (Nasicon) interface of the electrochemical sensor were investigated by means of complex impedance spectra in the frequency range 0.1 Hz–1 MHz and at the temperatures between 298 K and 873 K. A plausible equivalent circuit involving two *R*-CPE elements connected in series was proposed. The results were discussed in terms of the brick-layer model. The parameters characterizing Schottky barrier occurring at the grain boundary interface were determined.

Keywords: impedance spectroscopy, electrochemical gas sensors, solid electrolytes, Nasicon

1. Introduction

Solid electrochemical cells are well known devices used to monitor the concentration of many gases e.g. CO_2, SO_x and NO_x. The structure of a such sensor can in most cases be represented as [1–9]:

$$\text{Au, air} + \text{G, AP}|\text{Na}^+\text{—SE}|\text{ B, air, Pt} \qquad (1)$$

where G is the monitored gas (CO_2, SO_x or NO_x), AP is a gas-sensing material, termed as an "*auxiliary phase*". Carbonates, sulfates or nitrates of alkaline metals are used as an AP in such a sensor, accordingly to the type of gas that is monitored. Na^+—SE is a sodium containing solid electrolyte such as Nasicon and B is a material containing sodium phase with constant activity of Na_2O.

*To whom all correspondence should be addressed.

The output signal of the sensor is the electromotive force (EMF) of the solid cell (1). The EMF will be a simple function of concentration of monitored gas if the potential of reference electrode assumes a constant value and the local equilibria are established at the electrodes of the sensor. Unfortunately, literature data are rarely related to these conditions. The aim of this paper is to examine behaviors of both the reference electrode and solid electrolyte/reference electrode system of cell (1). A heterogeneous mixture TiO_2—$Na_2Ti_6O_{13}$ (6 : 1 molar ratio) reported in [3] was used as reference electrode.

2. Experimental Details

2.1. Materials Preparation

The sodium containing electrode was a heterogeneous mixture of $Na_2Ti_6O_{13}$ and TiO_2 (1:6 molar ratio) which

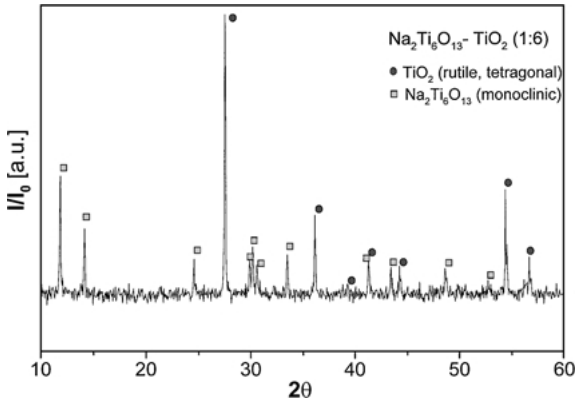

Fig. 1. XRD pattern of the specimen $Na_2Ti_6O_{13}$—TiO_2 (B).

was prepared from TiO_2 (anatase, provided by Cookson Technology Centre, UK) and Na_2CO_3 (ACS primary standard 99.95%, Sigma-Aldrich) by solid-state reaction. The appropriate amounts of powders were mixed, pressed into pellets and calcined at 1000°C for 24 hours. The product of the reaction was crushed in an agate mortar, milled, isostatically pressed into pellets at 200 MPa and sintered at 1100°C for 2 hours. Apart from the pellets, some powder was also sintered in order to obtain the material for preparation of a ceramic $Na_2Ti_6O_{13}$—TiO_2 paste, used later for the electrode formation. The pellets obtained were polished with a diamond paste to diameter of 11.0 mm and thickness of 1.8 mm, then cleaned in alcohol using an ultrasonic cleaner, dried at 100°C and stored in a desiccator until used for preparation of samples or further experiments.

Figure 1 shows the X-ray diffraction patterns of the obtained material, which is a two phase mixture of monoclinic $Na_2Ti_6O_{13}$ and TiO_2 (rutile). This result is in agreement with the phase diagram of this system published in Ref. [10]. The SEM image of the surface microstructure of the specimen is presented in Fig. 2. As can be seen, the material is composed of two types of irregular grains with different size. The energy dispersion X-ray analysis (EDX, Oxford Instruments, LINK ISIS 300) indicated clearly that smaller grains (average grain size $4.7 \pm 1.2\,\mu$m) are the TiO_2 rutile phase, while sodium enriched bigger grains are the $Na_2Ti_6O_{13}$ crystallites. The details of preparation and the properties of the solid electrolyte were described elsewhere [11].

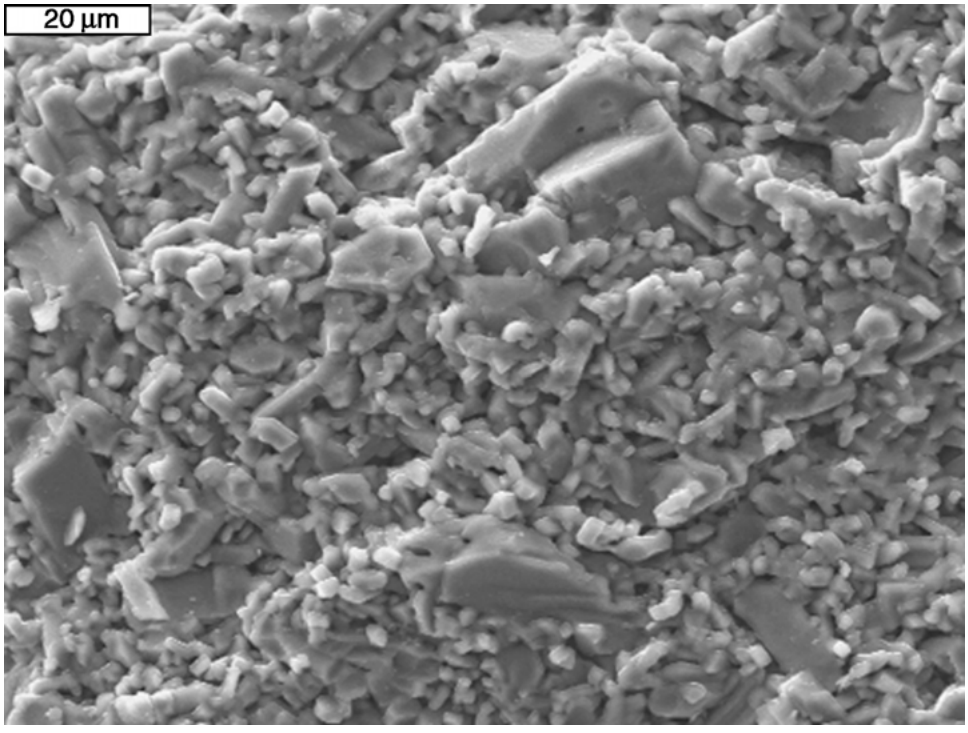

Fig. 2. SEM micrograph of the specimen B. Smaller and bigger grains correspond to TiO_2 (rutile) and $Na_2Ti_6O_{13}$ (monoclinic) phases, respectively.

Table 1. Sample characterization. Description of samples prepared for the impedance measurements.

Sample	Material	Electrodes (both side)
NB	Nasicon pellet	$Na_2Ti_6O_{13}$—TiO_2 (1 : 6) | Porous platinum
B	$Na_2Ti_6O_{13}$—TiO_2 (1 : 6) pellet	Porous platinum

2.2. *Electrode Formation*

Two samples labeled as NB and B were examined. Their composition is given in Table 1. The porous platinum electrodes were screen printed with the platinum paste (product of Demetron), dried at room temperature and fired at 900°C for 30 minutes. The sodium electrodes ($Na_2Ti_6O_{13}$—TiO_2 pellets) were attached to the Nasicon using the ceramic paste prepared from $Na_2Ti_6O_{13}$—TiO_2 powder suspended in organic solvent, dried at room temperature and fired at 900°C for 30 minutes.

2.3. *Impedance Measurements*

The impedance measurements were performed using an IM5d Impedance Spectrum Analyser (Zahner Electrik) in the frequency range 0.1 Hz–1 MHz. The amplitude of the sinusoidal voltage signal was 20 mV. All the measurements were carried out in air in the temperature range 298 K–873 K. The details concerning the experimental procedure and the sample holder are reported elsewhere [11].

3. Results and Discussion

3.1. *Analysis of Equivalent Circuits*

In the Z' vs. $-Z''$ coordinates the experimental spectra can be approximated by two semicircles as illustrated in Figs. 3 and 4. The circles radii decrease when the temperature is increasing. The equivalent circuit, whose response is used for fitting the impedance spectra, is shown in Fig. 5. The presence of two semicircles in Fig. 5 may be ascribed to either bulk and grain boundary properties or effect of heterogeneity of studied material. The first approach is based on the assumption that the large grains of one component in the solid mixture of $Na_2Ti_6O_{13}$—TiO_2 are connected to each other and only they have impact on the observed impedance spectra. Considering the structure of the sample presented in Fig. 2., $Na_2Ti_6O_{13}$ can be assumed to be a component

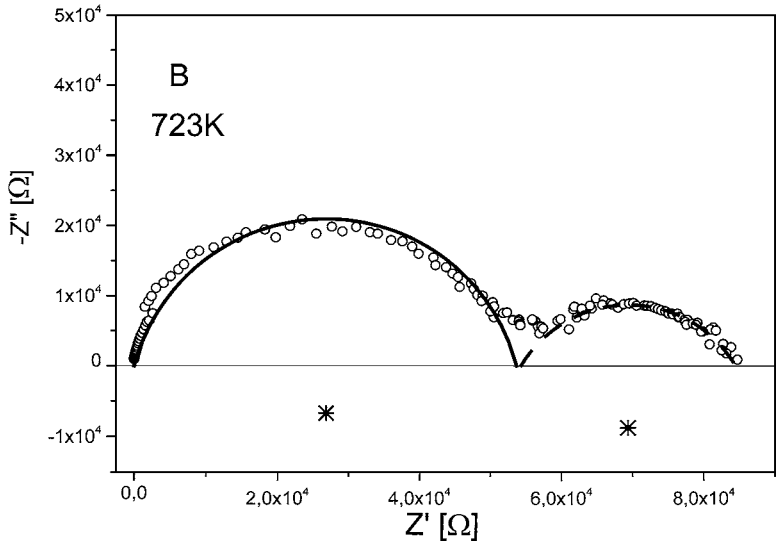

Fig. 3. Plot $-Z''$ vs. Z' for the sample B at 723 K.

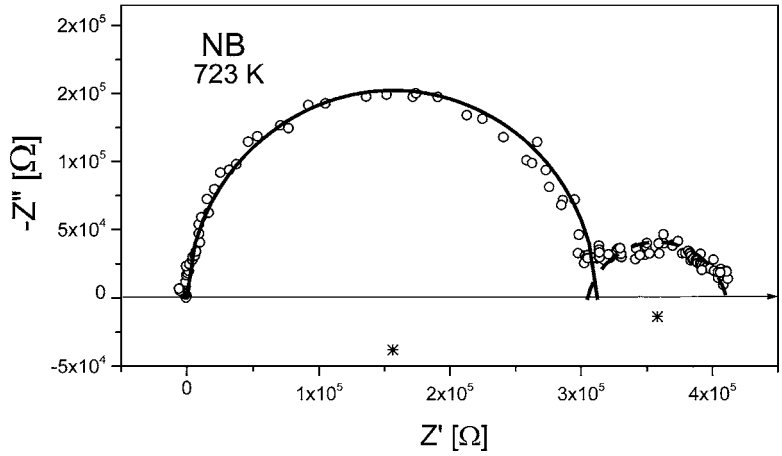

Fig. 4. Plot $-Z''$ vs. Z' for the sample NB at 723 K.

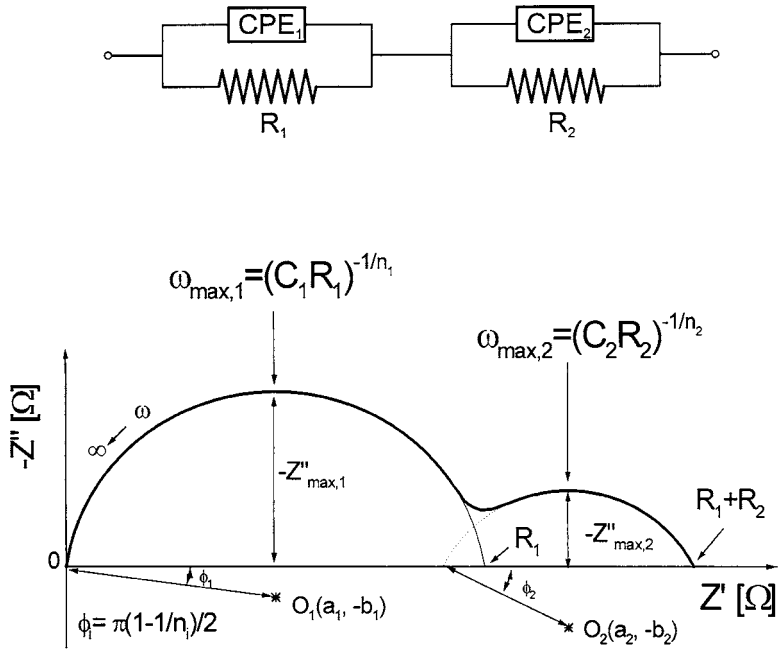

Fig. 5. Equivalent circuit and schematic representation of the chosen parameters at the impedance spectrum.

of this type. In such a case the R_1 and R_2, determined accordingly to the procedure shown in Fig. 5., correspond to the resistivity of bulk and grain boundary of the $Na_2Ti_6O_{13}$, respectively [12]. This case is called a '*homogeneous approach*'.

According to the second approach the determined parameters of the first and second semicircles are attributed to each of the two components of the sodium electrode material separately. Namely, R_1 and R_2 represent the resistivities of the $Na_2Ti_6O_{13}$ and TiO_2, respectively. This case is called a '*heterogeneous approach*'.

The mean effective capacitance, C_{mean}, can be estimated from the peak frequency $\omega_{\max}$ (which corresponds to the maximum value $-Z''$ of the response in Fig. 5) [12]:

$$C_{\text{mean}} = \frac{1}{R\omega_{\max}} \tag{2}$$

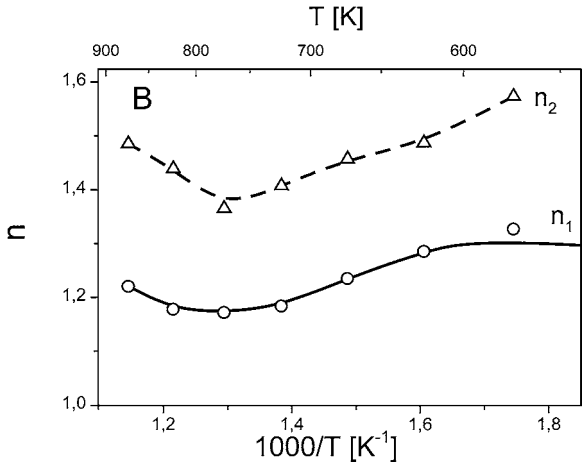

Fig. 6. Parameters n_1 and n_2 of the sample B as a function of reciprocal temperature.

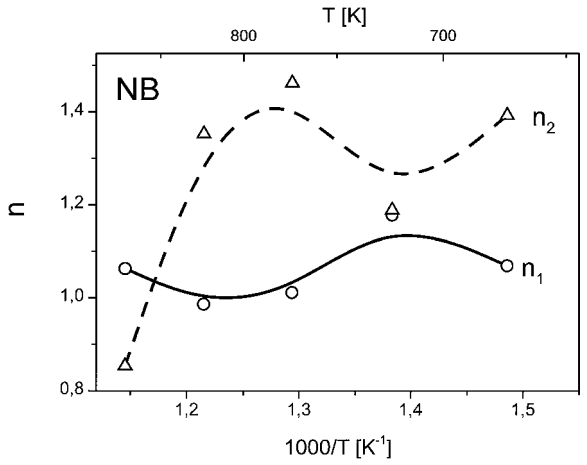

Fig. 7. Parameters n_1 and n_2 of the sample NB as a function of reciprocal temperature.

Figures 6 and 7 illustrate the temperature dependences of the n_1 and n_2 parameters, defined in Fig. 5, for the samples B and NB, respectively. Parameters n_1 and n_2 have the values between 1 and 2. The value $n = 1$ corresponds to the Debye capacitor. If $n = 2$, the *CPE* element represents the semi-infinite diffusion and is called the Warburg impedance [12]. As can be seen, the parameter n_1 is generally smaller than n_2 with one exception for the NB sample at the highest temperature.

The temperature dependences of the σ_1 and σ_2 conductivities are presented in Figs. 8 and 9. They were determined from the R_1 and R_2 taking into account the geometry and dimensions of the samples. The σ_2 appears to be higher than σ_1. The dependences of the capacitances determined by use of Eq. (2) on temperature are also shown in these figures. The C_1 capacitance has the value of several nF which is essentially independent on temperature. The C_2 values are 2–3 orders of magnitude higher than those of the C_1. In the case of NB sample, the C_2 increases with temperature.

Applying the brick-layer model of the studied ceramic material [12], the determined capacitances C_1 and C_2 allow to determine the ratio of thicknesses (d_2/d_1) of the media *"1"* and *"2"* (the grain boundaries thickness and grain size in the case of '*homogenous approach*' or grain sizes of two components in the case of '*heterogenous approach*'):

$$\frac{d_2}{d_1} = \frac{\varepsilon_2 C_1}{\varepsilon_1 C_2} \tag{3}$$

where ϵ_1 and ϵ_2 are the dielectric constants of the media *"1"* and *"2"*, respectively.

3.2. *Homogeneous Approach*

Assuming that the impedance spectra describe the $Na_2Ti_6O_{13}$ phase, the determined quantities n_i, σ_i, C_i with $i = 1, 2$ correspond to bulk ($i = 1$) and grain boundaries ($i = 2$). Taking into consideration that both the bulk and grain boundaries have similar chemical composition, an approximation $\epsilon_1 = \epsilon_2$ is usually assumed in the literature [12].

According to the Schottky barrier model for semiconducting junction [13] adapted also for solid electrolytes by Heyne [14], the Schottky space charge layer thickness is equal to a half of grain boundary thickness: $d_2/2$. On the other hand, the Schottky barrier potential, Φ_S may be expressed as:

$$\Phi_S = \frac{E_{\text{act},2} - E_{\text{act},1}}{2e} \tag{4}$$

where e is an elementary charge, $E_{\text{act},1}$ and $E_{\text{act},2}$ are the activation energies.

The average grain size of $Na_2Ti_6O_{13}$ was estimated on the basis of SEM image (Fig. 2.) to be $d_1 = 4.7\ \mu$m. Taking into account this value we can determine the thickness of the grain boundaries, d_2, using Eq. (3) and the Schottky barrier potential from Eq. (4). The determined parameters characterizing the space charge properties of the studied materials are listed in Table 2.

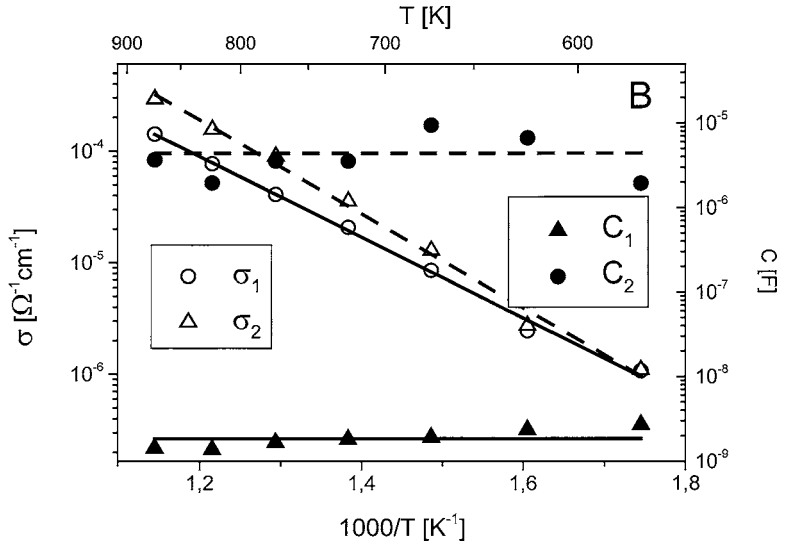

Fig. 8. Electrical conductivity and mean capacitance values of the bulk and grain boundary of the sample B as a function of reciprocal temperature.

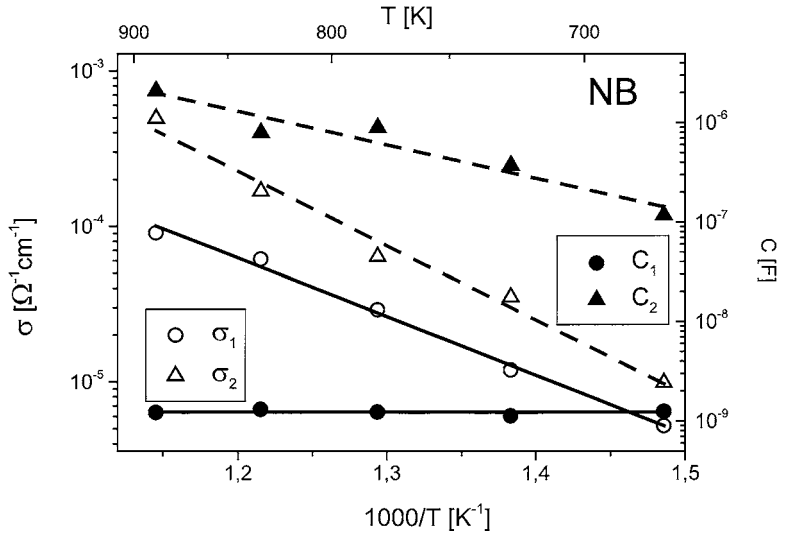

Fig. 9. Electrical conductivity and mean capacitance values of the bulk and grain boundary of the sample NB as a function of reciprocal temperature.

There is no available data in the literature concerning space charge in the studied materials. It is usually assumed, that the expected space charge layer thickness is equal to several nanometers. The experimentally determined space charge layer thickness for TiO_2 (rutile) by Ikuma and Komatsu [15] is equal to 4.5–20 nm. The larger values of the thickness determined for the NB in comparison with these found for the B, may be explained by an effect of the Nasicon phase on the studied impedance spectra.

3.3. Heterogeneous Approach

In this approach the media *"1"* and *"2"* are identified as the TiO_2 and $Na_2Ti_6O_{13}$ phases, or vice-versa. The

Table 2. Parameters characterizing space charge properties.

Sample	Schottky barrier potential (V)	Schottky space charge layer thickness (nm)	
		573 K	873 K
NB	0,1	39 ± 10	2.9 ± 0.7
B	0,06	1.96 ± 0.49	1.96 ± 0.49

electron microscopy observations revealed that the ratio d_2/d_1 is close to 1. Assuming the dielectric constant of TiO_2 amounts to 100 and 75 at 573 and 873 K, respectively [16], the dielectric constant of $Na_2Ti_6O_{13}$ determined from Eq. (3) is either (1.3–2.4) 10^5 (when subscripts 1 and 2 corresponds to TiO_2 and $Na_2Ti_6O_{13}$, respectively) or 0.03–0.9 (when subscripts 2 and 1 corresponds to TiO_2 and $Na_2Ti_6O_{13}$, respectively). Unfortunately, there are no available data of the dielectric constant for $Na_2Ti_6O_{13}$. However, most ceramic materials have the dielectric constant between 4 and 110 and only some perovskite titanates have value of the order 10^3 . This shows that proposed approach is inappropriate.

3.4. *Dependences of Electrical Conductivity on Temperature*

Figures 10 and 11 illustrate the dependences of $\log(\sigma T)$ on $1/T$ for both the B and NB samples. Taking into consideration that the activation energies

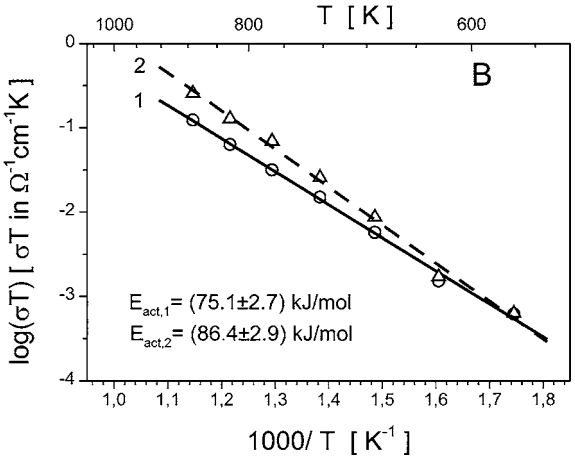

Fig. 10. Logarithm of $\sigma_1 T$ and $\sigma_2 T$ versus $1/T$ of the bulk and grain boundary conductivities of the sample B.

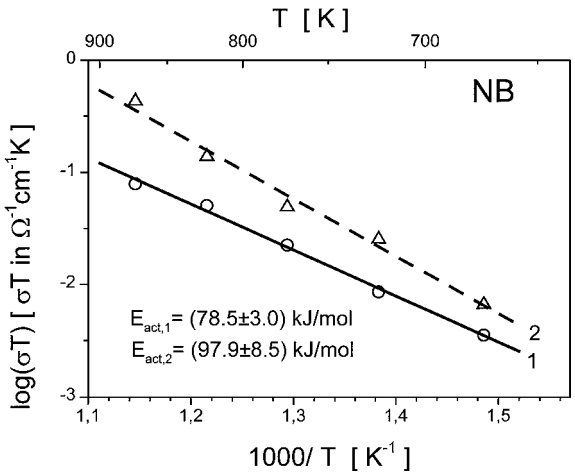

Fig. 11. Logarithm of $\sigma_1 T$ and $\sigma_2 T$ versus $1/T$ of the bulk and grain boundary conductivities of the sample NB.

(75.1 and 78.5 kJ/mol) are similar, but much higher than that of Nasicon [11], and the electrical conductivity is several orders of magnitude lower than that of Nasicon [11], we conclude that the determined electrical conductivity can be attributed to the presence of sample B. Since the activation energy of the TiO_2 component approaches the value about twice higher (146 kJ/mol) [17] than measured we conclude, that the electrical properties determined in this work are characteristic for the $Na_2Ti_6O_{13}$ component.

4. Conclusions

The electrical properties of the composite ($Na_2Ti_6O_{13}$—TiO_2)-Nasicon-($Na_2Ti_6O_{13}$—TiO_2) are close to those for $Na_2Ti_6O_{13}$—TiO_2. The impedance properties of $Na_2Ti_6O_{13}$—TiO_2 can be modeled well in terms of an electrical circuit containing the bulk and grain boundary elements in series. The conductivity of the grain boundary is higher than that of the bulk. Also, the activation energy of the grain boundary conductivity is higher than that of the bulk. Under the

assumption of brick-layer model we have determined the parameters characteristic for the space charge properties, i.e. the Schottky barrier potential and Schottky space charge layer thickness.

Acknowledgments

The financial support of Polish State Committee for Scientific Research (KBN), Project No. 7 T08A 037 15 is acknowledged.

References

1. K. Singh, P. Ambekar, and S.S. Bhoga, *Solid State Ionics*, **122**, 191 (1999).
2. Y.C. Zhang, H. Tagawa, S. Asakura, J. Mizusaki, and H. Narita, *J. Electrochem. Soc.*, **144**, 4345 (1997).
3. M. Holzinger, J. Maier, and W. Sitte, *Solid State Ionics*, **94**, 217 (1997).
4. D.J. Slater, R.V. Kumar, and D.J. Fray, *Solid State Ionics*, **86–88**, 1063 (1996).
5. T. Maruyama, Y. Saito, Y. Matsumoto, and Y. Yano, *Solid State Ionics*, **17**, 281 (1985).
6. S-D. Choi, W-Y. Chung, and D-D. Lee, *Sensors, and Actuators*, B **35/36**, 263 (1996).
7. N. Miura, M. Ono, K. Shimanoe, and N. Yamazoe, *Sensors and Actuators*, B **49**, 101 (1998).
8. Y. Shimizu and K. Maeda, *Sensors and Actuators*, B **52**, 84 (1998).
9. N. Miura, M. Iio, G. Lu, and N. Yamazoe, *Sensors and Actuators*, B **35/36**, 124 (1996).
10. R. Bouaziz and M. Mayer, *R.Sc Acad. Sci., Ser. C*, **272** (23), 1874 (1971).
11. P. Pasierb, S. Komornicki, R. Gajerski, S. Kozinski, P. Tomczyk, and M. Rekas, *J. Electroceramics*, **8**, 49 (2002).
12. J.R. Macdonald and D.R. Franceschetti, in *Impedance Spectroscopy*, edited by J.R. Macdonald (John Wiley & Sons, New York, 1987), p. 84.
13. H.K. Henisch, in *Semiconductor Contacts: An Approach to Ideas and Models* (Clarendon Press, Oxford, 1984), p. 43.
14. L. Heyne, in *Mass Transport in Solids*, edited by F. Beniere and C.R.A. Catlow (Plenum Press, New York, 1983), p. 425.
15. Y. Ikuma and W. Komatsu, *Ikutoku Kogyo Daigaku Kenkyu Hokoku*, B **8**, 187 (1984).
16. R.A. Parker, *Phys.Rev.*, **124**, 1719 (1961).
17. S. Komornicki, M. Radecka, and M. Rekas, *J. Mater. Sci. Electron. Materials*, **12**, 11 (2001).